

Carlosturanite, a new asbestiform rock-forming silicate from Val Varaita, Italy

ROBERTO COMPAGNONI

*Dipartimento di Scienze della Terra
Università della Calabria, Castiglione scalo, 87030 Cosenza, Italy*

GIOVANNI FERRARIS

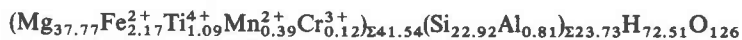
*Dipartimento di Scienze della Terra
Università di Torino, via S. Massimo 22, 10123 Torino, Italy*

AND MARCELLO MELLINI

*C.N.R., C.S. Geologia Strutturale Dinamica dell'Appennino
via S. Maria 53, 56100 Pisa, Italy*

Abstract

Carlosturanite is a new rock-forming silicate occurring in a network of veins crosscutting the antigorite serpentinite of Sampeyre in the Monviso ophiolite, Italy. It is light-brown, asbestiform, and the [010] fibers are paralleled by fibrous diopside and chrysotile. The mineral is monoclinic *Cm*, with $a = 36.70$, $b = 9.41$, $c = 7.291\text{\AA}$, $\beta = 101.1^\circ$. The strongest lines in the X-ray powder diffraction pattern are: 18.02(25)(200), 7.17(100)(001,201), 3.595(45)(10.00, 002), 3.397(55)(202), 2.562(40)(802), 2.280(35)(14.01,16.01). Similar refractive indices are measured along (1.605) and across (1.600) the fiber axis. Carlosturanite dehydrates upon heating, forming chrysotile and hematite (400°C) and finally forsterite (770°C). The infrared pattern shows absorption bands due to hydroxyl anions and silicate tetrahedra. Chemical data lead to the empirical chemical formula



($D_{\text{calc}} = 2.606$, $D_{\text{obs}} = 2.63\text{g/cm}^3$) or, ideally and according to a structural model, $\text{M}_{21}[\text{T}_{12}\text{O}_{28}(\text{OH})_4](\text{OH})_{30} \cdot \text{H}_2\text{O}$ ($Z = 2$). Carlosturanite or carlosturanite-like phases may be expected to develop in serpentinite compositions under low grade metamorphic conditions.

Introduction

Specimens of the new mineral were first collected on the working face of a chrysotile-asbestos mining prospect, located some 5 km west of Sampeyre (Val Varaita, Piedmont, Italy). The mine is situated in a metamorphic serpentinite belonging to a southern portion of the Monviso ophiolite, which is part of the internal Piemonte-Liguria Mesozoic ophiolitic belt, in the penninic domain of the Western Alps.

The new mineral strongly resembles fibrous serpentine, for which it can be mistaken in the field; it has commonly been called metaxite or metaxitic serpentine (Zucchetti, 1968) or xylotile, i.e., the same names used for balangeroite, another macroscopically similar fibrous silicate from Balangero (Lanzo Valley, Piedmont) described by Compagnoni et al. (1983).

The name carlosturanite is after Carlo Sturani (1938-1976), Professor of Geology at the University of Torino, whose untimely death occurred in a fatal accident during field work. The name and the species have been approved by the I.M.A. Commission on New Minerals and Mineral

Names. The holotype material is kept at the Museo Regionale delle Scienze (Torino).

Occurrence

Carlosturanite is quite common in the Sampeyre serpentinite, where it occurs over an area of a few square kilometers. The zone underwent a polyphase metamorphic evolution characterized by an Early Alpine event under greenschist facies conditions (Hunziker, 1974). Structural and mineralogical relics indicate that the antigoritic serpentinite derives from an upper-mantle spinel lherzolite partly re-equilibrated under the plagioclase peridotite facies, like most serpentinites of the ophiolitic belt of the Western Alps (Compagnoni et al. 1985).

Carlosturanite develops in a close network of veins (from 0.1 mm to several centimeters thick) randomly crosscutting the serpentinite (Fig. 1). Usually it occurs together with chrysotile, diopside, and opaque ore minerals (magnetite and native NiFe alloys); locally, clinohumite, perovskite, and a green uvarovite garnet are also found. Frequently,

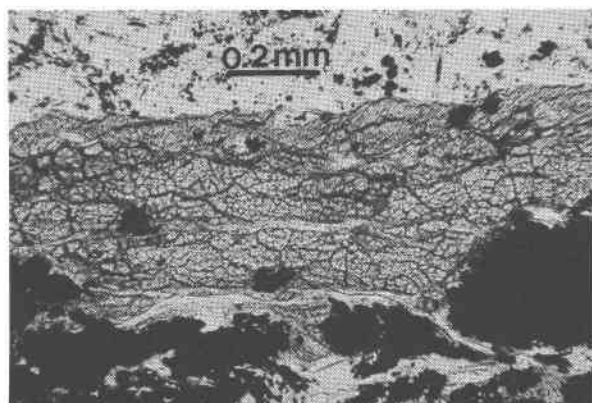
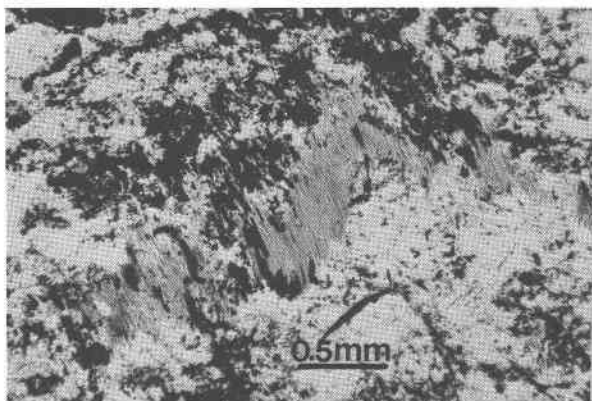


Fig. 1. Deformed vein (upper) and bundles (lower) of carlosturanite cut parallel and perpendicular to the fiber axis, respectively (plane polarized light).

the carlosturanite-bearing veins appear to have been deformed and/or reactivated several times, resulting in a complex structural and mineralogical texture. On the one hand these veins appear to be crosscut by the later monomineralic veins of antigorite, chrysotile, brucite, and magnesite; on the other hand they seem to reactivate or crosscut earlier veins of antigorite, of chrysotile and of olivine + clinohumite + diopside + opaques. Microscopic observations indicate that carlosturanite, as well as the other serpentine minerals, is frequently replaced by brucite. Transmission Electron Microscope (TEM) images, showing brucite crystals apparently pseudomorphic after single sturranite fibers and embayed by abundant chrysotile, suggest the following breakdown reaction: carlosturanite \rightarrow brucite + chrysotile.

Physical and crystallographic properties

Carlosturanite is light-brown, flexible, and develops [010] fibers several centimeters long, commonly gathered in folded bundles. The streak is whitish, and the luster is vitreous-pearly. The fibrous nature of the mineral prevent-

ed determination of the hardness. Parallel intergrowth between [010] carlosturanite, [001] diopside (Fig. 2), and [100] chrysotile fibers occurs in extremely variable degrees from macroscopic to TEM scale; at the latter scale brucite occurs in the presence of abundant chrysotile (Fig. 3). Single fibers of carlosturanite are seldom larger than 0.2 μm . Very good {001} cleavage and an approximate {010} fracture are observed. A density of 2.63(2) g/cm^3 was determined by the heavy liquid method.

Optical measurements are very difficult and imprecise. In thin section carlosturanite is transparent and pleochroic with orange brown and pale orange brown parallel and perpendicular to [010], respectively. The extinction is parallel and the elongation positive. Because of the texture, only an average refractive index, 1.600(5), has been observed perpendicular to [101]; 1.605(5) has been measured along [010]. Birefringence is low (first order orange) to very low (grey), though greyish-blue anomalous interference colors are locally shown by sections cut parallel to the fiber axis. Interference figures, performed on fiber bundles cut perpendicular to the fiber axis, are definitely positive, but may appear either pseudo-uniaxial or biaxial with small to moderate optic axial angle. Microscopically, carlosturanite is very similar to balangeroite, from which it may be distinguished by lower refractive indices ($n = 1.68$ in balangeroite) and by weaker pleochroism ($\alpha =$ pale yellowish red-brown and $\gamma =$ reddish brown in balangeroite).

Only the powder diffraction pattern and the repetition period along the fiber axis could be obtained by X-ray diffraction. The b -rotation photographs ($\text{CuK}\alpha$ radiation) show strong zero and third layer lines, all the other layer lines being definitely weak (Fig. 4); such a pattern can be compared with that of antigorite around b (Aruja, 1946) and of balangeroite around c (Compagnoni et al., 1983). Superposition of 5.2 \AA layer lines of chrysotile occurs with some samples. Only continuous lines are observed on the Weissenberg photographs, indicating complete rotational disorder around the elongation direction. Selected area electron diffraction patterns indicated $C2/m$, Cm , or $C2$ symmetry (Mellini et al., 1985) and supplemented the a , c , and β starting values used to index the powder diffraction pattern (Table 1); a least-squares unit cell refinement based on the powder data gave $a = 36.70(3)$, $b = 9.41(2)$, $c = 7.291(5)\text{\AA}$, and $\beta = 101.1(1)^\circ$. Because of the fibrous nature of the material, preferred orientation may affect the powder diffraction patterns. In particular, most reflections with $k \neq 0$ have been observed only with Guinier-Lenné camera; these reflections are starred in Table 1. Undoubtedly, the unit cell dimensions and the distribution of the strongest reflections recall the serpentine minerals (Whittaker and Zussman, 1956), but the overall powder pattern is definitely characteristic for carlosturanite. In particular, supplementary lower angle reflections (18.02 and 9.01 \AA) occur in the new mineral.

Thermal and infrared study

The weight loss at 1000 $^\circ\text{C}$, as determined by Thermogravimetric Analysis (TGA) (Fig. 5), is 16.85%. Comparison

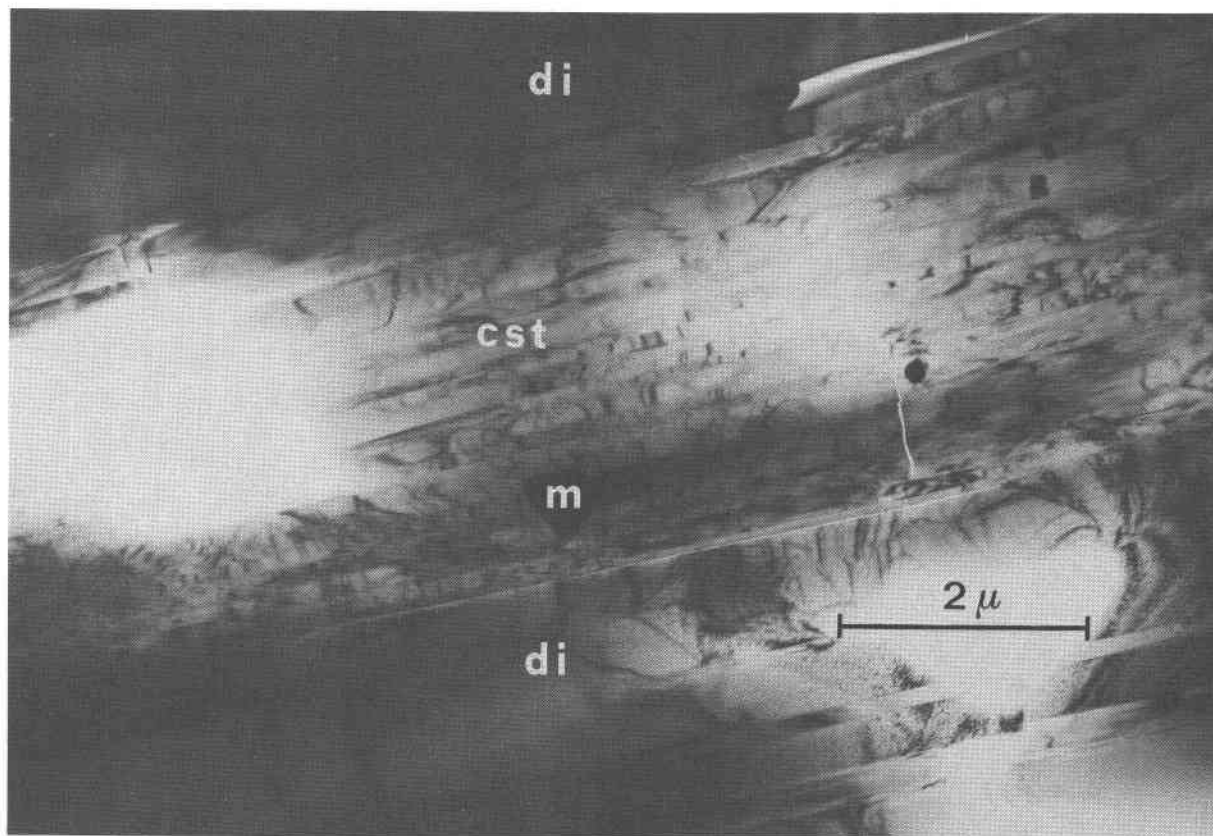


Fig. 2. TEM image of parallel intergrowth of diopside (di) and carlosturanite (cst). The opaque inclusion (m) is chromian magnetite.

with Differential Thermogravimetric Analysis (DTG) reveals that the weight loss begins at 40°C and continues quite smoothly with minor flexes at 75°C (1%), 105°C (1.8%) and 195°C (2.5%). After further loss to 5.6% at 380°C, a smoother slope begins, and then a step (600°C) brings the weight loss to 13% at 750°C; the last part of the curve has a flex at 900°C.

A continuous X-ray powder pattern recorded from 20 to 1100°C (20°C/hour) shows a practically constant pattern of carlosturanite up to about 400°C where it vanishes, leaving at least two other phases: a serpentine phase, which disappears at about 500°C, and hematite, which is still present at 1100°C. The latter is the only crystalline phase evident from 500 to 700°C, when forsterite appears. Minor shifts of lines towards higher angles can be detected around 200°C. Keeping in mind the different rates of heating, the two different high-temperature experiments can be regarded as consistent with one another.

The infrared spectrum (Fig. 6) displays absorption bands due to the presence of hydroxyl anions and silicate tetrahedra; as a whole, it is similar to that of chrysotile, with major differences in the low frequency side of the SiO₄ stretching vibrations between 950 and 850 cm⁻¹. The wide range observed for the temperature of dehydration, starting

just above room temperature, suggests that H₂O may be present as well.

Compositional data

Table 2 reports the average results of fifteen electron microprobe analyses obtained by wavelength dispersive analysis on a fully automated ARL-SEM-Q instrument, using olivine (Si, Mg, Fe), jadeite (Al), ilmenite (Ti), Mn-hortonolite (Mn), and Cr-garnet (Cr) as standards; H₂O is from TGA. No other element with Z > 11 was shown by TEM/EDS analyses. Some variation, particularly for the minor constituents, was detected with the microprobe; this variation is probably due to submicroscopic intergrowths or to the heterogeneities discussed in the companion paper by Mellini et al. (1985). Determination of Fe³⁺ was not attempted. On the basis of 126 oxygen atoms per unit cell (see below) the following empirical formula was derived: (Mg_{37.77}Fe_{2.17}Ti_{1.09}Mn_{0.39}Cr_{0.12})_{Σ41.54}(Si_{22.92}Al_{0.81})_{Σ23.73}H_{72.51}O₁₂₆. From this formula D_{calc} = 2.606 g/cm³ is obtained with F.W. = 3873.45. The Gladstone-Dale relationship gives K = 0.229 compared with 0.230 calculated from the empirical formula with Mandarino's (1976) refractivities.

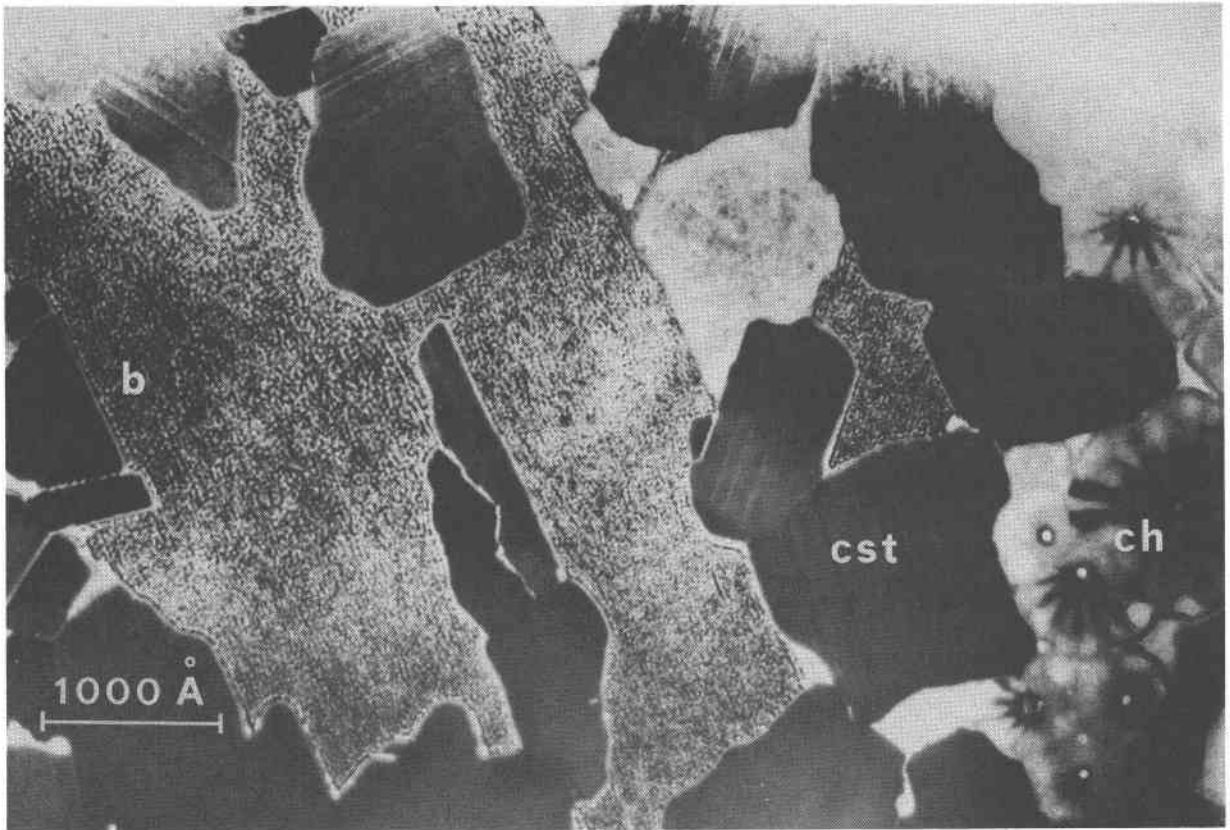


Fig. 3. TEM image showing association of fibrous carlosturanite (cst), brucite (b) and chrysotile (ch) as seen along the fiber axis.

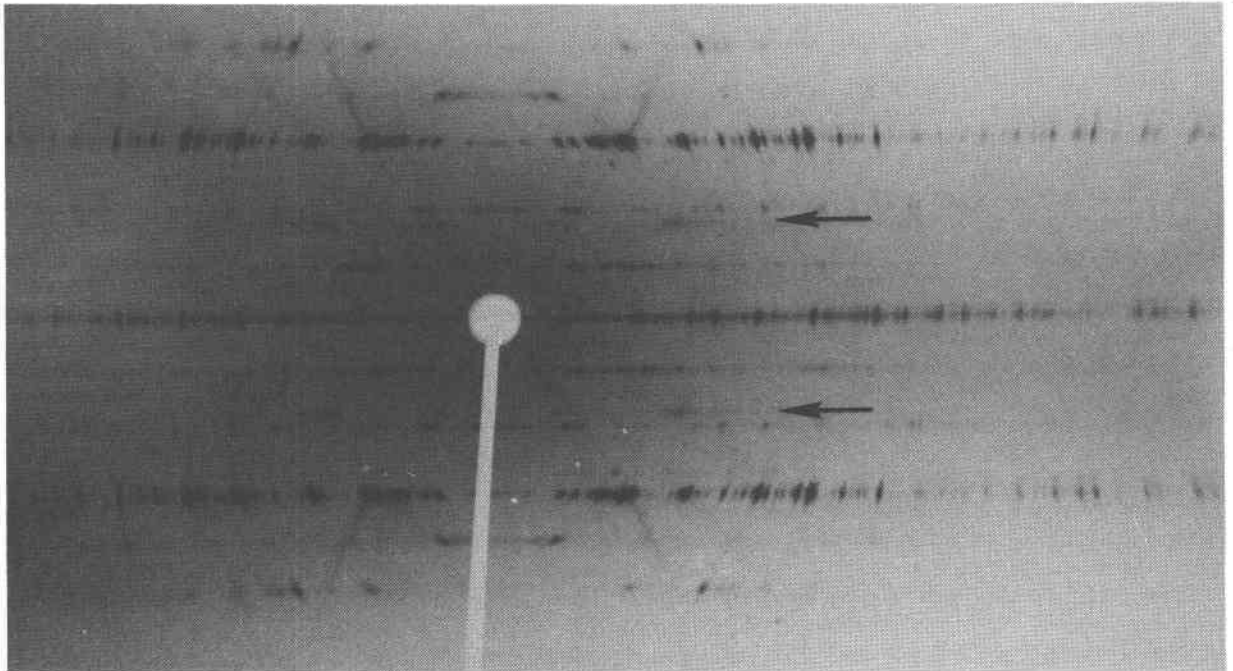


Fig. 4. *b*-rotation photograph of carlosturanite (Ni-filtered CuK α radiation). The 5.2 Å layer lines of intergrown chrysotile are shown by arrows.

Table 1. X-ray powder data for carlosturanite, obtained by powder diffractometer and Guinier-Lenné camera (CuK α radiation). Intensities (I_0) on relative scale, observed (d_o) and calculated (d_c) interplanar spacings with their assigned hkl indices are reported. Starred d_o values refer to reflections that are observed only in Guinier-Lenné patterns.

I_0	d_o (Å)	d_c (Å)	hkl
25	18.02	18.01	200
5	9.01	9.00	400
100	7.17	7.16; 7.14	001; $\bar{2}01$
10	6.28	6.25; 6.21	201; 401
5	5.67	5.76; 5.72; 5.50	$\bar{1}11$; 510; 111
15	5.15	5.14; 5.11	401; 601
5	4.22	4.22; 4.19	601; 801
10	4.71*	4.71	020
20	3.637	3.645	$\bar{2}02$
45	3.595	3.601; 3.578	10 \cdot 00; 002
10	3.513	3.518; 3.498	801; $\bar{1}0\cdot01$
55	3.397	3.387	202
15	3.096	3.106	$\bar{8}02$
5	2.988	3.001; 2.994; 2.979	12 \cdot 00; 10 \cdot 01; $\bar{1}2\cdot01$
5	2.849	2.844; 2.843	$\bar{3}31$; 602
5	2.818	2.824	$\bar{1}0\cdot02$
5	2.674*	2.678	730
15	2.586	2.584	$\bar{1}4\cdot01$
40	2.562	2.571	802
20	2.539	2.553	$\bar{1}2\cdot02$
10	2.425	2.424; 2.424; 2.426	$\bar{9}31$; 403; $\bar{2}03$
10	2.308	2.308	203
15	2.293	2.298	803
35	2.280	2.285; 2.276	14 \cdot 01; $\bar{1}6\cdot01$
5	2.101*	2.109; 2.101	12 \cdot 02; 15 \cdot 11
10	2.065*	2.067; 2.065	17 \cdot 10; 823
10	1.9373	1.9452; 1.9280	$\bar{1}4\cdot03$; 932
15	1.9223	1.9212; 1.9211	14 \cdot 02; 333
5	1.9030	1.9096	15 \cdot 30
5	1.8170	1.8147; 1.8123	$\bar{2}04$; 604
15	1.7098*	1.7117; 1.7081	18 \cdot 21; 10 \cdot 23
15	1.6030	1.6024	14 \cdot 03
20	1.5679*	1.5683	060
5	1.3995	1.4005; 1.3968	$\bar{1}2\cdot05$; $\bar{2}4\cdot03$
5	1.3671	1.3671; 1.3675	$\bar{1}4\cdot05$; $\bar{1}7\cdot34$
5	1.2835	1.2854; 1.2813	16 \cdot 04; 463
5	1.2790	1.2768; 1.2790	$\bar{2}4\cdot04$; $\bar{1}0\cdot63$

Crystal chemistry

Carlosturanite a , b , and c lattice parameters closely correspond to $7a$, b , and c of the fundamental serpentine orthorhombic cell. On the basis of this relationship, the other described properties, and further high-resolution TEM results, a structural model is proposed by Mellini et al. (1985). It is based on the serpentine structure with the tetrahedral sheet split into strips consisting of [010] triple silicate chains which result from introduction of ordered vacancies. According to this model, the empirical formula of carlosturanite can be written (Mg, Fe, Ti, Mn, Cr, \square) $_{21}$ [(Si, Al) $_{12}$ O $_{28}$ (OH) $_4$](OH) $_{30}$ ·H $_2$ O with two formula units per unit cell; brackets enclose the silicate polyanion. In light of this formula, the thermal behavior of carlosturanite can be interpreted according to the following steps: (1) loss of H $_2$ O (\approx 1%) and of the (OH) $^-$ in the silicate strip

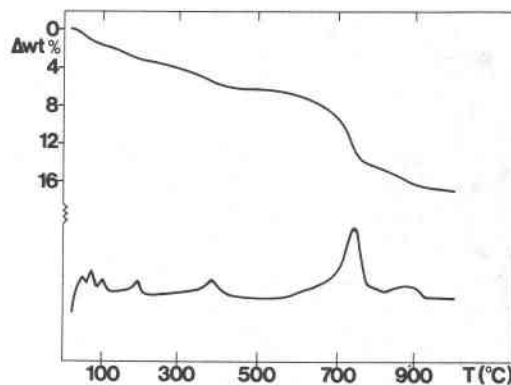


Fig. 5. TGA (top) and DTG (bottom) curves in air; 5.25 mg of carlosturanite at a rate of 20°C/min.

(a further 1.9%) without collapse of the structure (cf. the shrinkage of the unit cell at about 200°C); (2) breaking of the inter-strip octahedra with loss of (OH) $^-$ and release of the corresponding cations; (3) formation of hematite and, possibly, of other undetected oxides; (4) condensation of the strips to form a serpentine phase; (5) collapse of this phase with formation of forsterite. Steps (2), (3) and (4) are simultaneous. The exact balance of the weight loss in the steps (2) and (3) cannot be determined theoretically, in view of the unknown cation content of the broken octahedra (see below). In any case, the weight loss at the end of step (3) cannot exceed the corresponding TGA value measured at the temperature of the formation of hematite.

The appearance of hematite with serpentine means that iron is released at this stage, presumably together with other cations: in fact, the 2.2 Fe atoms of the empirical formula are not sufficient to fill the six inter-strip octahedra per unit cell that must be broken to form serpentine (cf.

Table 2. Electron microprobe analysis of carlosturanite. H $_2$ O determined by TGA.

	1	2
MgO	36.7 - 41.3	39.28
FeO	3.2 - 5.8	4.03
TiO $_2$	1.0 - 4.1	2.24
MnO	0.5 - 1.2	0.72
Cr $_2$ O $_3$	0.2 - 0.3	0.24
SiO $_2$	33.9 - 37.2	35.53
Al $_2$ O $_3$	1.0 - 1.3	1.07
H $_2$ O	-	16.85
Total		99.96

1. Min/max % weights for 15 electron microprobe analyses.

2. Average % weight.

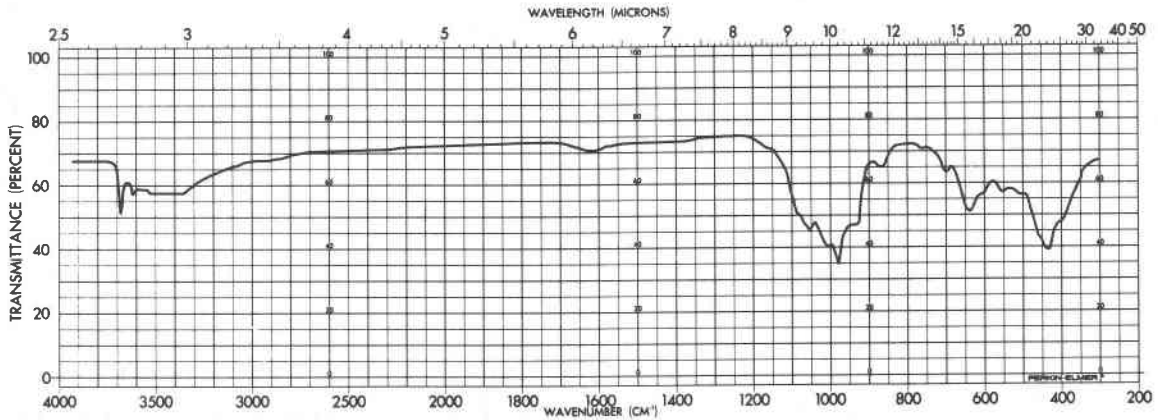


Fig. 6. Infrared spectrum of carlosturanite (KBr disk).

Fig. 3 in Mellini et al., 1985). Since the cations other than Mg can have ionization numbers higher than 2 and their sum is smaller than 6, a plausible hypothesis is that they are located in the inter-strip octahedral sites, where some vacancies also should be present to compensate the highly charged cations.

Conclusions

Carlosturanite, a major constituent of the serpentinite from Sampeyre, is found to be closely related to the serpentine minerals in its physical and chemical properties and probable formation conditions and phase equilibria. It can be defined as a Si-poor, highly-hydrated, serpentine-like phase. Most probably, carlosturanite, or carlosturanite-like phases, are not rare and may be found in many similarly metamorphosed serpentinites. In fact, a search of old literature data on serpentine (Hintze, 1897; Dana, 1914) shows several cases of Si-poor and H₂O-rich analyses that recall the composition of carlosturanite. In some cases "species names" such as hydrophite and enophite (Dana, 1914) were proposed as well. However, identification of such occurrences as carlosturanite is not possible, because definitive diffraction data are not available.

Textural evidence suggests that carlosturanite, chrysotile, and fibrous diopside grew together, forming a stable mineral assemblage. The stability field of diopside + chrysotile is considered to lie approximately between 250 and 300°C at $P_{\text{liquid}} = P_{\text{H}_2\text{O}} = 2$ kbar (Trommsdorff, 1983); therefore, similar very low grade metamorphic conditions may be suggested also for carlosturanite. Within the diopside + chrysotile stability field, the growth of carlosturanite possibly is controlled by chemical parameters. Among them, a significant role may be played by Ti. In fact, this element is a pervasive constituent of carlosturanite, while systematically absent from the associated minerals (Mellini et al., 1985).

Acknowledgments

The authors are grateful to Professor E. Occeila (Dipartimento di Georisorse e Territorio, Politecnico di Torino), who called our

attention to the fibrous mineral and supplied us with the first specimen. Professors R. Rinaldi and A. Alberti (Istituto di Mineralogia e Petrografia dell'Università di Modena) kindly performed electron microprobe and TGA/DTG analyses, respectively.

References

- Aruja, E. (1946) An X-ray study of the crystal-structure of antigorite. *Mineralogical Magazine*, 27, 65–74.
- Compagnoni, R., Ferraris, G. and Fiora, L. (1983) Balangeroite, a new fibrous silicate related to gageite from Balangero, Italy. *American Mineralogist*, 68, 214–219.
- Compagnoni, R., Piccardo, G. B., and Sandrone, R. (1985) Ophiolites from the Western Alps and the Apennines. In N. Bogdanov, Ed., *Ophiolites of Continents and Comparable Oceanic Floor Rocks*. Elsevier, in press.
- Dana, E. S. (1914) *The System of Mineralogy of J. D. Dana*. John Wiley, New York.
- Hintze, C. (1897) *Handbuch der Mineralogie*. Verlag Von Veit, Leipzig.
- Hunziker, J. C. (1974) Rb–Sr and K–Ar age determinations and the alpine tectonic history of the Western Alps. *Memorie dell'Istituto di Geologia e Mineralogia dell'Università di Padova*, 31, 1–54.
- Mandarino, J. A. (1976) Gladstone–Dale relationship—Part I: Derivation of new constants. *Canadian Mineralogist*, 14, 498–502.
- Mellini, M., Ferraris G., and Compagnoni, R. (1985) Carlostranite: HRTEM evidence of a polysomatic series including serpentine. *American Mineralogist*, 70, 773–781.
- Trommsdorff, V. (1983) Petrologic aspects of serpentinite metamorphism. *Rendiconti della Società Italiana di Mineralogia e Petrologia*, 38, 549–559.
- Whittaker, E. J. W., and Zussman, J. (1956) The characterization of serpentine minerals by X-ray diffraction. *Mineralogical Magazine*, 31, 197–126.
- Zucchetti, S. (1968) Mineralizzazioni nichelifere a ferro-nichel e solfuri nel giacimento asbestifero di Sampeyre (Cuneo) ed in altre serpentinitine alpine. *Bollettino della Associazione Mineraria Subalpina*, 5, 106–120.